Available online at www.eccomasproceedia.org
Eccomas Proceedia EUROGEN (2023) 324-332

ECCOMAS
Proceedia

EUROGEN 2023
15th ECCOMAS Thematic Conference on
Evolutionary and Deterministic Methods for Design, Optimization and Control
N. Gauger, K. Giannakoglou, M. Papadrakakis, J. Periaux (eds.)
Chania, Crete Greece, 1–3 June 2023

A MULTI-SCALE TOPOLOGY OPTIMIZATION APPROACH WITH IMPLICIT FUNCTION-BASED MICRO-STRUCTURES

Andrea Nale[1]*, Andrea Chiozzi[2]

[1] Department of Architecture
University of Ferrara
Via della Ghiara, 36 - 44121 Ferrara, Italy
andrea.nale@unife.it

[2] Department of Environmental and Prevention Sciences
University of Ferrara
C.so Ercole I d'Este, 32 - 44121 Ferrara, Italy
andrea.chiozzi@unife.it

Abstract

Topology optimization is a design method that afford an optimal layout with the minimization of a function, which describe a functional aspect, under prescribed constraints. The most common problem analysed in topology optimization is the compliance minimization, i.e. maximization of stiffness, under prescribed volume constraint. Here, we propose a multiscale approach with multi-material formulation where several microstructures, which differ in terms of material and topology, are generated using an implicit function. This approach, based on the theory of homogenization, allows to account for different microstructures and enables to obtain functionally graded structures. Several numerical examples are shown to illustrate the main features and advantages of the proposed multi-scale topology optimization approach.

Keywords: topology optimization, multi-scale approach, implicit function method

Peer-review under responsibility of the organizing committee of EUROGEN 2023.
doi: 10.7712/140123.10208.18926

1 INTRODUCTION

Topology optimization has gained increasing interest in various fields of engineering over the last decade. Despite structural optimization being developed throughout the 20th [1] and 21st [2] centuries, its practical implementation was constrained to theory due to difficulties in manufacturing the optimized layout. However, additive manufacturing has provided an opportunity to overcome the limitations of conventional manufacturing techniques. Therefore, in civil engineering, topology optimization has become a valuable tool to find and explore new solutions. This computational tool finds his power in the combination of a typical solution method used in the field of engineer, i.e. the Finite Element Method (FEM), which enables the attainment of a material distribution within a domain [3]. The optimal layout is determined by topology optimization with the distribution of holes and links in the structure by removing and adding material in the defined domain, with supports and loads, to satisfy specific constraints. In this paper, the proposed topology optimization uses a continuous approach, where a material model allows to intermediate values of a specific property, e.g. density of material, using a continuous parameter, which is the design variable, that determines the distribution of material and void. The most common material model adopted in topology optimization is the so-called density methods [3]. In particular, the traditional SIMP (Solid Isotropic Material with Penalization) model is widely used for its rather simple approach giving quality results. In this approach, a weighting function operates on the variables ρ inside a radius r_{min}, which shows the local nature of this operation. This approach is called also two-field SIMP, because the optimization algorithm uses both a design variable and a weighted density variable $\overline{\rho}$. An evolution of the SIMP method is given by the homogenization-based method [4], which recently received widespread interest due to the complexity, the scale, and connectivity of microstructural geometries. Indeed, these issues represented a key limitation for decades in favor of the solid isotropic material interpolation. The development of new technologies, i.e. additive manufacturing, revive this approach enabling the manifacturing of multi-material structure and hierarchical structures, e.g. periodic microstructures structures [5]. The multiscale structures, which are composed by microstructures with different geometries giving mechanical properties that vary spatially, recently received a great attention for the comparison to many natural structures and materials, such as bone and bamboo [6] [7], achieving compelling functionalities [8] that, in a general sense, promise superior performances. This contribution aims to outline a three-dimensional topology optimization approach for large-scale additive manufacturing to incorporates different microstructures. The structure of this paper is shown as follows. Section 2 presents the methodology, paying attention of the formulation proposed, the sensitivity analysis, the update scheme and multiscale approach adopted; Section 3 presents some examples of microstructures generated with the implicit function method and the conceptual idea of the approach. Finally in Section 4 conclusions and the future perspectives are given.

2 METHODOLOGY

The proposed topology optimization is a homogenization-based multi-scale approach with a multi-material formulation for a volume-constrained compliance minimization. The discrete problem statement for an elastic body is described as:

$$\min_{\mathbf{z}\in\left[\underline{\rho},\overline{\rho}\right]^{Nxm}} f = \mathbf{F}^T\mathbf{U} \text{ subject to}$$
$$g_j = \frac{\sum_{i\in G_j}\sum_{l\in\mathcal{E}_j} \mathrm{V}_l m_V}{\sum_{l\in\mathcal{E}_j} V_l} - \overline{v}_j \le 0, j = 1,...,K \tag{1}$$

where f is the objective function which is minimized under g_j constraints.
In the proposed approach the objective function f refers to the compliance, i.e. maximization of stiffness matrix, which is defined by multiplying the vector of applied loads **F** with the element displacements **U**. While the constraint is represented by the function g_j, $j = 1,...,K$, represent the volume for each volume constrain. The volume constraint restricts the selection of candidate materials in any specific subregion of the domain with the sets $\mathcal{E}_j$ and G_j that represent, respectively, the element and material indices related to constraint *j*. Moreover, V_l, $l = 1,...,N$, represents the volume, $m_V = y_{li}$ is the volume interpolation and the constraint is given by the volume limits $\overline{v}_j$.
The microstructure properties are embedded by the material volume v_{li}, $i = 1,...m$ for each candidate material, and the local stiffness matrix $\mathbf{k}_l$. In particular, the material volume $v_{li} = y_{li}\hat{v}_i$ incorporates the material porosity, through the unit cell volume $\hat{v}_i$, while y_{li} assigns the presence of an element and, if present, designates the candidate material to each of the N element centroids that make up the discretized domain. Ω.

$$\mathbf{k}_l = m_M\left(\mathbf{w}_l'\right) = \sum_{i=1}^{m} w_{li} \prod_{\substack{j=1 \\ j\neq i}}^{m}\left(1-\gamma w_{lj}\right)\mathbf{k}_{li}^0, l = 1,...,N \tag{2}$$

where m_M is interpolation function that penalizes the mixing of materials [9] and depends on the penalized element densities w_{li}, $\mathbf{k}_{li}^0$ is the element stiffness matrix and γ is the mixing penalty parameter. The penalized element density is defined as:

$$w_{li} = m_W\left(y_{li}\right) = y_{li}^p \tag{3}$$

with *p* a penalty parameter to penalize intermediate densities.
The local stiffness matrix is computed as:

$$\left(\mathbf{k}_{li}^0\right) = \int_{\Omega_l} \mathbf{B}_j^T\mathbf{D}_i^H\mathbf{B}_k d\mathbf{x} \tag{4}$$

where **B** describes the strain-displacement matrix of shape function derivates, Ω_l is the domain of element *l* and $\mathbf{D}_i^H$ is the homogenized material elasticity matrix, represented in Voigt notation, used as input for each material
The candidate material is determined by the implicit function-based modelling approach [10]. Indeed, this method is particularly useful to described porous structures by using implicit functions. Indeed, a function of cosine and sine, e.g. Fourier series, allows to defined a field

$\phi(\mathbf{x})$, which is defined by the points $\mathbf{x} \in \Omega$ of a domain $\Omega \subset \mathbb{R}^3$, and applying a threshold $\phi_{levelset}$ is possible to subdivided Ω into two subspaces:

$$\phi(\mathbf{x}) = \begin{cases} < \phi_{levelset} & \text{if } \mathbf{x} \text{ inside} \\ = \phi_{levelset} & \text{if } \mathbf{x} \text{ on the boundary} \\ > \phi_{levelset} & \text{if } \mathbf{x} \text{ outside} \end{cases} \tag{5}$$

and assigning to each subspace, according to a discrete level set function, the final solid-void assignment of each point:

$$\delta_l(\mathbf{x}_l) = \begin{cases} 1 \text{ if } \phi_l(\mathbf{x}_l) \geq \phi_{levelset} \\ 0 \text{ otherwise} \end{cases} \tag{6}$$

The computational homogenization [11] is carried out using a hexahedral mesh with 100 x 100 x 100 elements. This method allows us to handle any type of material and consider its effective macroscopic properties in the optimization process.
A gradient-based method is employed to solve the compliance minimization stated as Eq. (1). It involves the objective and constraint sensitivities with respect to the design variables. These are computed as following:

$$\frac{\partial f}{\partial \mathbf{z}_i} = \frac{\partial \mathbf{y}_i}{\partial \mathbf{z}_i} \frac{\partial \mathbf{w}_i}{\partial \mathbf{y}_i} \frac{\partial f}{\partial \mathbf{w}_i}, i = 1, \ldots, m \tag{7}$$

$$\frac{\partial g_j}{\partial z_i} = \frac{\partial \mathbf{y}_i}{\partial \mathbf{z}_i} \frac{\partial \mathbf{V}_i}{\partial \mathbf{y}_i} \frac{\partial g_j}{\partial \mathbf{V}_i}, j = 1, \ldots, K \tag{8}$$

and the individual contributes are:

$$\frac{\partial \mathbf{y}_i}{\partial \mathbf{z}_i} = \mathbf{P}^T \tag{9}$$

$$\frac{\partial f}{\partial w_{li}} = -\mathbf{U}^T \frac{\partial \mathbf{K}}{\partial w_{li}} \mathbf{U}, \frac{\partial w_{kj}}{\partial y_{li}} = \begin{cases} p y_{li}^{p-1}, & \text{if } l = k \text{ and } j = i \\ 0, & \text{otherwise} \end{cases} \tag{10}$$

$$\frac{\partial g_j}{\partial v_{li}} = \frac{\mathrm{A}_l}{\sum_{l \in \varepsilon_j} \mathrm{A}_l}, \frac{\partial v_{kj}}{\partial y_{li}} = \begin{cases} \hat{v}_i, & \text{if } l = k \text{ and } j = i \\ 0, & \text{otherwise} \end{cases} \tag{11}$$

$$\frac{\partial \mathbf{k}_k}{\partial w_{li}} = \begin{cases} \prod_{\substack{j=1 \\ j \neq i}}^{m} \left(1 - \gamma w_{lj}\right) \mathbf{k}_{li}^0 - \sum_{\substack{p=1 \\ p \neq i}}^{m} \gamma w_{lp} \prod_{\substack{r=1 \\ r \neq p \\ r \neq i}}^{m} \left(1 - \gamma w_{lr}\right) \mathbf{k}_{lp}^0, & \text{if } l = k \\ 0, & \text{otherwise} \end{cases} . \tag{12}$$

where $\mathbf{P}$ is the density filter matrix.

The sensitivities $\frac{\partial f}{\partial \mathbf{z}_i}$ and $\frac{\partial g_j}{\partial z_i}$ allow the implementation of the Zhang-Paulino-Ramos Jr. (ZPR) update scheme [12], where a series of convex approximate subproblem is solved using the Lagrange duality. The computation of these sensitivities allows to determine the candidate design variable:

$$z_{li}^{*} = \underline{\rho} + \left(B_{li}\right)^{\frac{1}{1+\alpha}} \left(\sum_{k=1}^{N} P_{lk} z_{ki}^{0} - \underline{\rho} \right) \tag{13}$$

where:

$$B_{li} = -\frac{\left.\frac{\partial f}{\partial z_{li}}\right|_{\mathbf{z}=\mathbf{z}^k}}{\lambda_j \left.\frac{\partial g_j}{\partial z_{li}}\right|_{\mathbf{z}=\mathbf{z}^k}}. \tag{14}$$

and he Langrange multipliers λ_j, at *k*-iteration, is evaluated solving with the bisection method the equation:

$$g_j\left(z_{li}^{k}\right) + \sum_{i \in M_j} \frac{\partial g_j}{\partial z_{li}} \left(z_{li}^{k}\right)^{T} \left(z_{li}\left(\lambda_j\right) - z_{li}^{k}\right) = 0. \tag{15}$$

The candidate design variable is accepted if respect the following box constraints:

$$z_{li}^{-} = \max\left(\underline{\rho}, z_{li}^{0} - M\right), z_{li}^{+} = \min\left(\overline{\rho}, z_{li}^{0} + M\right) \tag{16}$$

where $\underline{\rho}$ and $\overline{\rho}$ are respectively the maximum and minimum value allowable and M the move limit. So, the design variable at the new iteration is expressed as:

$$z_{li}^{new} = \begin{cases} z_{li}^{+}, z_{li}^{*} \geq z_{li}^{+} \\ z_{li}^{-}, z_{li}^{*} \leq z_{li}^{+} \\ z_{li}^{*}, \text{otherwise} \end{cases}. \tag{17}$$

3 RESULTS

The candidate materials produced through the implicit function method can vary by adjusting the weighted sum of cosine and sine functions. Some examples have been showed by Yang et. al. [13] and fabricated polymeric porous materials with stereolithography technique. Here, it is reported some cells [14] with unitary edge boundary (*a=b=c=1*) generated using the implicit-function model approach:

Morphology	Implicit Function	Model
Primitive	$\phi(\mathbf{x}) = cos\left(\frac{2\pi n_x}{a}x\right) + cos\left(\frac{2\pi n_y}{b}y\right) + cos\left(\frac{2\pi n_z}{c}z\right)$	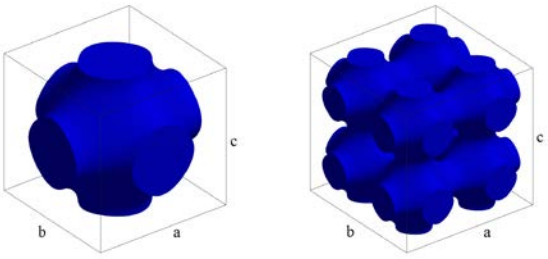
Gyroid	$\phi(\mathbf{x}) = cos\left(\frac{2\pi n_x}{a}x\right)sin\left(\frac{2\pi n_x}{a}y\right) + cos\left(\frac{2\pi n_y}{b}y\right)sin\left(\frac{2\pi n_y}{b}z\right) + cos\left(\frac{2\pi n_z}{c}z\right)sin\left(\frac{2\pi n_z}{c}x\right)$	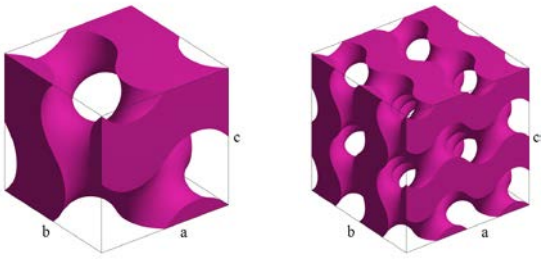
		$n_x = n_y = n_z = 1$ $\quad$ $n_x = n_y = n_z = 2$

Table 1: Periodic microstructures generated with implicit function method

The material properties, e.g. stiffness elasticity tensor $\mathbf{D}_i$, for topology optimization have been defined through homogenization [11]:

Isotropic	Primitive	Gyroid
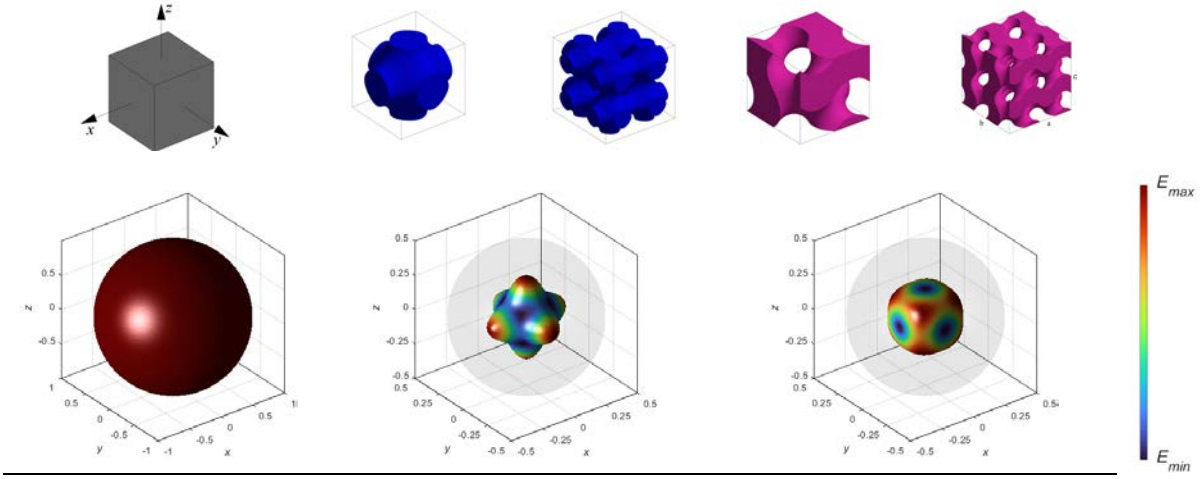		

Table 2: Elastic surfaces that indicate the tensile modulus direction dependence.

The material transition between cells is allowed with an interpolation function of the phase fields associate with each candidate material according to:

$$\phi_l(\mathbf{x}_l) = \frac{\sum_{i=1}^{m} max\left[0,1-\frac{d_{min}(\mathbf{x}_l, S_i)}{R_\phi}\right]^{1/2} \phi_{li}^0(\mathbf{x}_l)}{\sum_{i=1}^{m} max\left[0,1-\frac{d_{min}(\mathbf{x}_l, S_i)}{R_\phi}\right]^{1/2}} \tag{18}$$

where R_ϕ is the distance of the interpolation, $d_{min}(\mathbf{x}_l, S_i)$ is minimum distance between a generic point $\mathbf{x}_l$ the generic set S_i, $i = 1,...,m$, which contains all point $l \in S_i$, and $\phi_{li}^0(\mathbf{x}_l)$ represent the discrete version of the candidate material *m* phase field.
The presented method is currently being implemented for a 3D cantilever beam with a unit load *P* applied vertically at the tip and boundary fixed at the extreme (blue regions in Figure 1). The entire domain will be subject to volume constraints, with each constraint controlling a single material, to prevent any one microstructure from dominating the others.

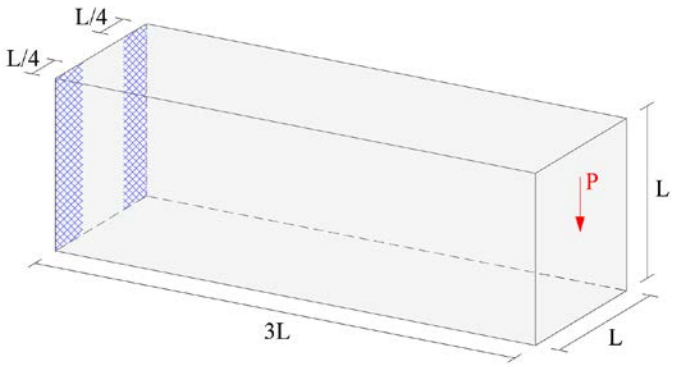

Figure 1: Cantilever beam domain and boundary conditions

The proposed approach has been applied for an isotropic material:

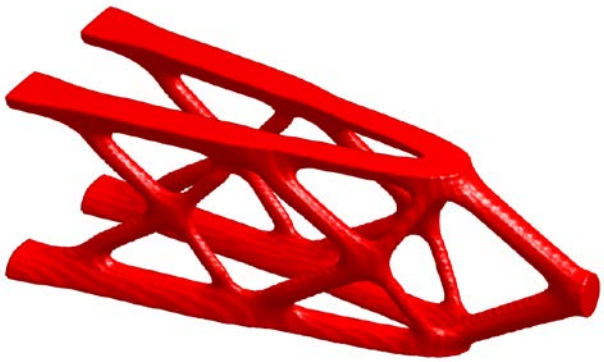

Figure 2: Cantilever beam optimized with isotropic material

In the same way, this method is ongoing to be applied for multiple periodic microstructures. It is expected to yield an optimized layout that share some geometric similarities to those seen in isotropic materials. In the following image, it is reported a conceptual depiction of the optimized layout obtained using the proposed methodology:

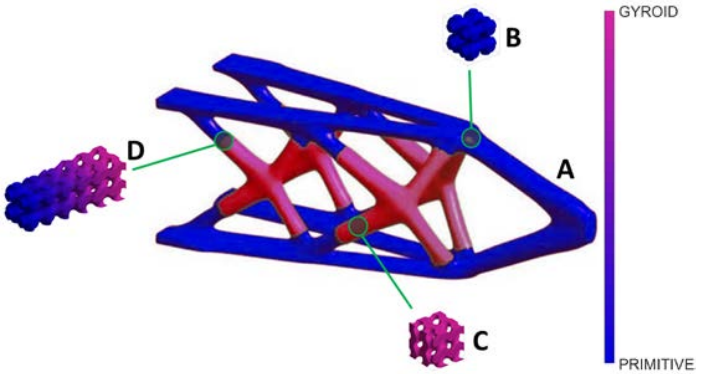

Figure 3: Conceptual representation of the result attended by the proposed method. The optimized layout in (**A**) with the microstructures (**B**) and (**C**), respectively Primitive and Gyroid cell. In (**D**) the cell transition with an interpolation function Eq. (18) on the phase fields of cells.

4 CONCLUSIONS

This work represents the starting point, whose objective is the topological optimization of structures with predefined cells structures to produce hierarchical civil structure components through large-scale additive manufacturing techniques. The next phases of this work will focus on developing the proposed optimization method and extending it with more appropriate formulation that consider the material features to suit civil engineering components, as well as on post-processing the structures for manufacturing purposes.

5 REFERENCES

[1] Topping BHV (1983) Shape optimization of skeletal structures: A review. J Struct Eng 109(8):1933–1951

[2] Rozvany GIN (2009) A critical review of established methods of structural topology optimization. Struct Multidiscip Optim 37(3): 217–237

[3] Bendsoe, M. P., and Sigmund, O. (2003). Topology optimization: theory, methods, and applications. Springer Science & Business Media.

[4] Sigmund O (1997) On the design of compliant mechanisms using topology optimization. Mech Struct Mach 25(4):493–524

[5] Wu, J., Sigmund, O., and Groen, J. P. (2021). Topology optimization of multi-scale structures: a review. Structural and Multidisciplinary Optimization, 63(3), 1455-1480.

[6] Lakes R (1993) Materials with structural hierarchy. Nature 361(6412):511–515.

[7] Fratzl P,Weinkamer R (2007) Nature's hierarchical materials. ProgMater Sci 52(8):1263–1334.

[8] U. G. Wegst, H. Bai, E. Saiz, A. P. Tomsia, R. O. Ritchie, Bioinspired structural materials. Nat. Mater. 14, 23–36 (2015).

[9] Sanders E. D., Pereira A., Aguiló M. A. and Paulino G. H. (2018). PolyMat: an efficient Matlab code for multi-material topology optimization. Structural and Multidisciplinary Optimization, 58, 2727-2759.

[10] Wang J., Rai R. and Armstrong J. N. (2020). Investigation of compressive deformation behaviors of cubic periodic cellular structural cubes through 3D printed parts and FE simulations. *Rapid Prototyping Journal*, *26*(3), 459-472.

[11] Hassani B. and Hinton E. (2012). Homogenization and structural topology optimization: theory, practice and software. Springer Science & Business Media.

[12] Zhang X. S., Paulino G. H. and Ramos A. S. (2018). Multi-material topology optimization with multiple volume constraints: a general approach applied to ground structures with material nonlinearity. Structural and Multidisciplinary Optimization, 57, 161-182.

[13] Yang N., Du C. F., Wang S., Yang Y. and Zhang, C. (2016). Mathematically defined gradient porous materials. Materials Letters, 173, 136-140.

[14] Sychov M. M., Lebedev L. A., Dyachenko S. V. and Nefedova L. A. (2018). Mechanical properties of energy-absorbing structures with triply periodic minimal surface topology. Acta Astronautica, 150, 81-84.